Electronic Supplementary Material (ESI) for Physical Chemistry Chemical Physics.

ELECTRONIC SUPPLEMENTARY INFORMATION

NMR chemical shift of confined ^{129}Xe: Coordination number, paramagnetic channels and molecular dynamics in a cryptophane-A biosensor

Perttu Hilla, Juha Vaara

perttu.hilla@oulu.fi; juha.vaara@iki.fi

NMR Research Unit
P.O. Box 3000, FI-90014 University of Oulu, Finland

Contents

List of Tables

List of Figures

1 Relativistic effects

To ensure that the contribution arising from the spin-orbit (SO) interaction to the NMR chemical shift (CS) δ of Xe is not significant for the conclusions in the present work, we computed for each system (i-iii, see the main text) three snapshots in the GFN-FF MD trajectory that lead to high, medium or low/negative Xe CS at the X2C [1, 2] level in the Turbomole programme [3, 4], using the 4-component DKS [5] level in the ReSpect programme [6]. Two calculations where the spin-orbit interaction was turned on/off were carried out for each snapshot. For the two XBS(aq) systems, water molecules were removed from the snapshots as their inclusion would have made the 4-component calculations unfeasible. The B3LYP exchange-correlation functional was used. The results are presented in Table S1.

Table S1: Comparison between the scalar-relativistic X2C level of theory and fully relativistic DKS level of theory in producing the NMR chemical shift (CS) δ, for Xe in the three environments (i-iii, see the main text). Results for three snapshots (SS1 – SS3) for each system are shown. The spin-orbit (SO) interaction has been turned on/off to study its contribution to the CS at the relativistic 4-component level. In the effects section, the average ("Avg.") value over the three snapshots of the 4-component correction, as well as the SO contribution, are shown. The different systems are colour coded as in the main text.

			Xe(aq)			XeCrA(aq)			XeWsCrA(aq)	
	Level of theory	**SS1**	**SS2**	**SS3**	**SS1**	**SS2**	**SS3**	**SS1**	**SS2**	**SS3**
Chemical shift δ	*X2C/BHandHLYP*	67.8	215.8	338.3	17.7	81.7	260.4	-11.8	30.2	243.1
	X2C/B3LYP	85.6	251.0	391.2	39.7	114.4	302.4	10.4	52.9	276.9
	DKS/B3LYP (SO On)	91.2	256.2	394.1	36.9	114.5	301.1	10.3	50.9	272.2
	DKS/B3LYP (SO Off)	91.8	255.1	390.4	38.0	116.4	303.0	10.8	51.9	274.6
Effects	*4c correction*	5.6	5.1	3.0	-2.8	0.0	-1.4	0.0	-2.0	-4.7
	Avg.		4.6			-1.4			-2.2	
	SO contribution	-0.5	1.0	3.7	-1.0	-1.9	-2.0	-0.5	-1.0	-2.4
	Avg.		1.4			-1.6			-1.3	

It can be seen that on average the SO interaction accounts for at most *ca.* ±2 ppm in computing the Xe CS, rendering its contribution negligible in the conclusions made in the main text. By looking at the 4-component correction row, the different sign in the deviation of the present computations from the experimental Xe CS values for Xe(aq) and XBSs(aq) can be seen to arise (at least partially) from the approximative, scalar relativistic treatment that was used in the main part of the present work. Fully relativistic treatment increases the Xe CS for Xe(aq) by about 5 ppm, resulting in a correction that would lead to very good agreement with experiment. For the XBS(aq) systems, the relativistic correction accounts for a decrease of about 2 ppm, which in the case of Xe@WsCrA(aq) would again result in very good agreement with experiment.

However, the limited selection of only three snapshots that were used in the above comparison should be kept in mind. Nevertheless, the observed trend may be expected to be the same if more snapshots were included.

2 Cluster extraction and basis set

To choose (1) the cut-off radius r_c that determines the number of water molecules included in the quantum-chemical calculations for Xe CS in the systems (i-iii), and (2) the basis-set level for the environment, a set of calculations with systematic improvement to points (1) and (2) were performed. In point (1), starting from $r_c = 5$ Å and 6 Å for (i) and (iii), respectively, calculations with increments of $\Delta r_c = 0.5$ Å were done at the MHA/x2c-SVPall [7] level. CS differences to clusters with $r_c = 5$ Å and 0 Å (the latter corresponding to no solvent around the cage) for (i) and (iii), respectively, are plotted against r_c in Fig. S1.

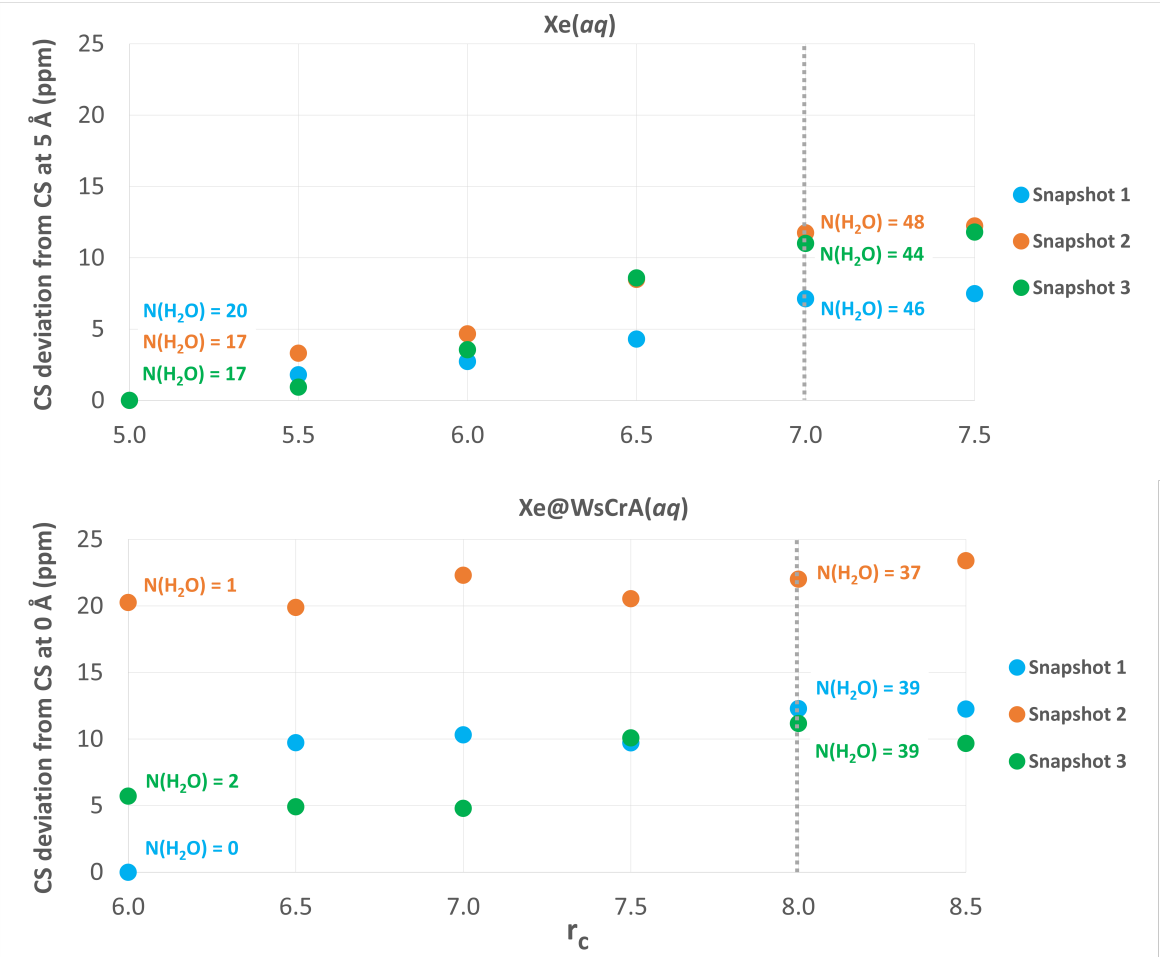

Figure S1: Deviations in Xe CS from the situations of $r_c = 5$ Å and 0 Å as a function of r_c for the two systems Xe(aq) and Xe@WsCrA(aq), respectively. Results for three different low-energy snapshots from the GFN-FF MD trajectory are shown.

It is seen that the inclusion of explicit solvent molecules can induce a change of up to *ca.* 20 ppm in the case of Xe@WsCrA. The CS converges to a 2-ppm window around the radii 7 Å and 8 Å for Xe(aq) and Xe@WsCrA(aq), respectively, and these were chosen as the final cut-off radii to be used in the motional averaging of Xe CS.

The effect of improving the basis set applied for the environment of Xe [point (2)] is shown in S2. Starting from $r_c = 5$ Å and 6 Å for Xe(aq) and Xe@WsCrA(aq), respectively,

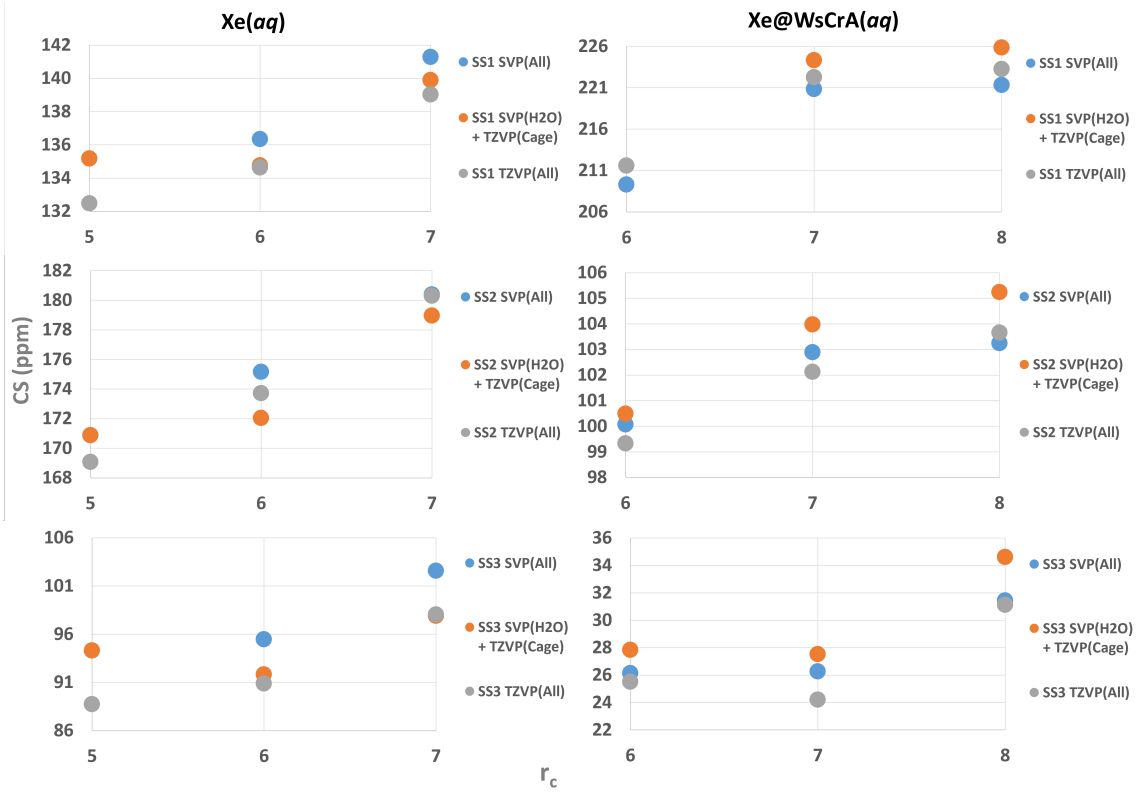

Figure S2: Xe CS as a function of r_c and the level of basis set applied for the environment of Xe. Three snapshots (SS1 − SS3) for the two systems Xe(aq) and Xe@WsCrA(aq) are shown.

three snapshots with cluster increments of $\Delta r_c = 1$ Å were studied. For each cluster, the basis set was improved from x2c-SVPall for every atom in the environment [SVP(All) in S2], to x2c-TZVPall basis for the WsCrA cage only [SVP(H2O) + TZVP(Cage)], and finally to x2c-TZVPall for the entire environment. It is seen that at the final cut-off radii, improving the basis set produces no systematic improvement on the CS results. For both systems and for each snapshot, the maximum difference between the Xe CS predicted by the three different basis sets is no more than 5 ppm, which (especially since this is not a systematic change) is a negligible source of error for the motional averaging of Xe CS in the main part of the work. Hence, x2c-SVPall was chosen to maximize the computational efficiency.

3 Resources used

The resulting number of water molecules in each cluster was, on average, 40 to 50. Hence, the final system sizes for producing the trajectory-averaged Xe CS were *ca.* 150 atoms for Xe(aq), and 250 atoms for the Xe@CrA(aq) and Xe@WsCrA(aq) systems, resulting in a total of 1500 − 3000 basis functions at the MHA/x2c-SVPall level. The multipole-accelerated RIJ scheme [8–10] was used, which practically completely retains the precision of the results while improving computational efficiency. In the end, the total wall time for the shielding calculations with 128 AMD Rome CPUs for one snapshot, using the

above-presented workflow, was *ca.* 10 min and 1 h for systems (i) and (ii-iii), respectively. For the three systems (i-iii) the number of included snapshots (as determined by the computational resources and the length of the available MD trajectory) were 64 (with 4 ps sampling interval), 128 (4 ps) and 64 (4 ps) at the GFN2 level, 208 (5 ps), 256 (8 ps) and 128 (5 ps) at the GFN0 level, and 1024 (2.5 ps), 512 (5 ps) and 512 (5 ps) at the GFN-FF level.

References

(1) D. Peng, N. Middendorf, F. Weigend and M. Reiher, *J. Chem. Phys.*, 2013, **138**, 184105.

(2) Y. Franzke and F. Weigend, *J. Chem. Theory Comput.*, 2019, **15**, 1028–1043.

(3) *TURBOMOLE V7.5.1, a development of University of Karlsruhe and Forschungszentrum Karlsruhe GmbH, 1989-2007*, 2020, `http://www.turbomole.com`.

(4) S. G. Balasubramani et al., *J. Chem. Phys.*, 2020, **152**, 184107.

(5) S. Komorovský, M. Repisky, O. Malkina, V. Malkin, I. Ondík and M. Kaupp, *J. Chem. Phys.*, 2008, **128**, 104101.

(6) M. Repisky, S. Komorovsky, M. Kadek, L. Konecny, U. Ekström, M. Kaupp, K. Ruud, O. Malkina and V. Malkin, *J. Chem. Phys.*, 2020, **152**, 184101.

(7) P. Pollak and F. Weigend, *J. Chem. Theory Comput.*, 2017, **13**, 36963705.

(8) K. Eichkorn, O. Treutler, H. Öhm, M. Häser and R. Ahlrichs, *Chem. Phys. Lett.*, 1995, **240**, 283–290.

(9) K. Eichkorn, F. Weigend, O. Treutler and R. Ahlrichs, *Theor. Chem. Acc.*, 1997, **97**, 119–124.

(10) M. Sierka, A. Hogekamp and R. Ahlrichs, *J. Chem. Phys.*, 2003, **118**, 9136–9148.